Nonlinear Dynamic Response of a Wind Turbine Rotor under Gravitational Loading

Inderjit Chopra* and John Dugundji†
Massachusetts Institute of Technology, Cambridge, Mass.

Abstract

THE nonlinear equations of motion for an isolated 3-deg flapping-lagging-feathering rotor blade are derived using Lagrange's equations for arbitrary large angular deflections. The aerodynamic forces and the tower interaction are not considered here. A consistent set of nonlinear equations is obtained by using nonlinear terms up to third order.

The limit cycle analysis for forced oscillations and the principal parametric resonance of the flap-lag blade under a periodic gravity field are studied using the harmonic balance method. For a relatively small initial coning angle (about 9 deg), the nonlinearity becomes of the softening spring type, and large coupled responses are possible for rotational frequencies significantly lower than the lagging frequency.

Contents

Figure 1 presents the blade configuration. A particular hinge sequence of feathering θ first, flapping β second, and lagging ϕ last is followed. It is assumed that there is no offset of the c.g. from the feathering axis and that the blade is uniform spanwise. The stiffness of the blade is represented by three springs at the hinge point representing, respectively, the flapping, lagging, and feathering motions.

By use of Lagrange's equations, the equations of motion are derived in Ref. 1 for a rotating blade with arbitrary large angular deflections. These are

$$\begin{aligned}
&\ddot\theta[(I_\xi\cos^2\phi+I_\eta\sin^2\phi)\cos^2\beta+I_\zeta\sin^2\beta]+\tfrac{1}{2}\ddot\beta(I_\eta-I_\xi)\cos\beta\sin2\phi-\ddot\phi I_\zeta\sin\beta-\dot\theta\dot\beta(I_\xi\cos^2\phi+I_\eta\sin^2\phi-I_\zeta)\sin2\beta+\dot\theta\dot\phi(I_\eta-I_\xi)\\
&\quad\times\cos^2\beta\sin2\phi-\tfrac{1}{2}\dot\beta^2(I_\eta-I_\xi)\sin\beta\sin2\phi+\dot\beta\dot\phi[(I_\eta-I_\xi)\cos2\phi-I_\zeta]\cos\beta+\dot\theta(2\zeta_\theta\sqrt{I_\xi k_\theta})+\Omega\dot\beta[(I_\eta-I_\xi)\sin\theta\sin\beta\sin2\phi\\
&\quad+(I_\xi\sin^2\phi+I_\eta\cos^2\phi)\cos\theta+(I_\xi\cos^2\phi+I_\eta\sin^2\phi-I_\zeta)\cos\theta\cos2\beta]+\Omega\dot\phi[I_\zeta\sin\theta\cos\beta+(I_\eta-I_\xi)(\tfrac{1}{2}\cos\theta\sin2\beta\sin2\phi\\
&\quad-\sin\theta\cos\beta\cos2\phi)]+\tfrac{1}{2}\Omega^2[(I_\xi\cos^2\phi+I_\eta\sin^2\phi\sin2\phi)\sin2\theta\sin^2\beta-(I_\xi\sin^2\phi+I_\eta\cos^2\phi)\sin2\theta+(I_\eta-I_\xi)\cos2\theta\sin\beta\sin2\phi\\
&\quad+I_\zeta\cos^2\beta\sin2\theta]+k_\theta(\theta-\theta_s)=gS_\zeta\sin\psi(\cos\theta\sin\beta\cos\phi+\sin\theta\sin\phi)
\end{aligned}\tag{1}$$

$$\begin{aligned}
&\ddot\beta(I_\xi\sin^2\phi+I_\eta\cos^2\phi)+\tfrac{1}{2}\ddot\theta(I_\eta-I_\xi)\cos\beta\sin2\phi+\dot\theta\dot\phi[(I_\eta-I_\xi)\cos\beta\cos2\phi+I_\zeta\cos\beta]-\dot\beta\dot\phi(I_\eta-I_\xi)\sin2\phi+\dot\theta^2(I_\xi\cos^2\phi\\
&\quad+I_\eta\sin^2\phi-I_\zeta)\tfrac{1}{2}\sin2\beta-\Omega\dot\theta[(I_\xi\sin^2\phi+I_\eta\cos^2\phi)\cos\theta+(I_\xi\cos^2\phi+I_\eta\sin^2\phi-I_\zeta)\cos\theta\cos2\beta+(I_\eta-I_\xi)\sin\theta\sin\beta\sin2\phi]\\
&\quad+\dot\beta(2\zeta_\beta\sqrt{I_\eta k_\beta})+\Omega\dot\phi[(I_\eta-I_\xi)(\sin2\phi\sin\theta+\cos2\phi\cos\theta\sin\beta)+I_\zeta\cos\theta\sin\beta]+\tfrac{1}{2}\Omega^2[I_\zeta\cos^2\theta\sin2\beta-(I_\xi\cos^2\phi+I_\eta\sin^2\phi)\\
&\quad\times\cos^2\theta\sin2\beta+(I_\eta-I_\xi)\tfrac{1}{2}\sin2\theta\cos\beta\sin2\phi+2eS_\zeta\sin\beta\cos\phi]+k_\beta(\beta-\beta_s)=gS_\zeta[\sin\psi\sin\theta\cos\beta\cos\phi-\cos\psi\sin\beta\cos\phi]
\end{aligned}\tag{2}$$

$$\begin{aligned}
&\ddot\phi I_\zeta-\ddot\theta I_\zeta\sin\beta-\dot\theta\dot\beta[(I_\eta-I_\xi)\cos\beta\cos2\phi+I_\zeta\cos\beta]-\dot\theta^2(I_\eta-I_\xi)\tfrac{1}{2}\cos^2\beta\sin2\phi+\dot\beta^2(I_\eta-I_\xi)\tfrac{1}{2}\sin2\phi+\Omega\dot\theta[(I_\eta-I_\xi)\\
&\quad\times(\sin\theta\cos\beta\cos2\phi-\tfrac{1}{2}\cos\theta\sin2\beta\sin2\phi)-I_\zeta\sin\theta\cos\beta]+\dot\phi(2\zeta_\phi\sqrt{k_\phi I_\zeta})-\Omega\dot\beta[(I_\eta-I_\xi)(\sin\theta\sin2\phi+\cos\theta\sin\beta\cos2\phi)\\
&\quad+I_\zeta\cos\theta\sin\beta]+\tfrac{1}{2}\Omega^2[(I_\eta-I_\xi)(\sin^2\theta\sin2\phi-\cos^2\theta\sin^2\beta\sin2\phi+\sin2\theta\sin\beta\cos2\phi)+2eS_\zeta\cos\beta\sin\phi]+k_\phi(\phi-\phi_s)\\
&\quad=gS_\zeta[-\sin\psi(\sin\theta\sin\beta\sin\phi+\cos\theta\cos\phi)-\cos\psi\cos\beta\sin\phi]
\end{aligned}\tag{3}$$

In these equations, I_ξ, I_η, I_ζ are the blade mass moment of inertias at the hinge about the feathering, flap, and lag axes, respectively. The k_θ, k_β, k_ϕ are the spring stiffnesses, and θ_s, β_s, ϕ_s are the initial settings for spring moments. The constant g is the gravity parameter, and S_ζ is the static unbalance about the hinge ($=\tfrac{1}{2}m\ell^2$). The ζ_θ, ζ_β, ζ_ϕ are the structural damping coefficients, and Ω is the rotation speed of the blade which is assumed to be fixed here. Also note that $\psi=\Omega t$.

The full equations of motion can be simplified somewhat by expanding the trigonometric terms up to third order, i.e.,

$$\sin\alpha\approx\alpha-(1/6)\alpha^3;\quad \cos\alpha\approx 1-\tfrac{1}{2}\alpha^2 \tag{4}$$

and also noting for these blades that $I_\xi \ll I_\eta$ and $I_\zeta \simeq I_\eta + I_\xi$. After considering terms up to third order, a consistent set of nonlinear equations is obtained.[1]

In the present paper, the dynamic response of the flapping-lagging blade under gravitational excitation is studied using the harmonic balance method. The equations of motion for

Received Aug. 29, 1977; synoptic received Jan. 19, 1978; revision received April 12, 1978. Full paper available from National Technical Information Service, Springfield, Va., 22151 as N78-15565 at the standard price (available upon request).

Index categories: Wind Power; Helicopters; Structural Dynamics.

*Research Assistant; presently NRC Research Associate, NASA Ames Research Center, Moffett Field, Calif.

†Professor, Aeronautics and Astronautics. Member AIAA.

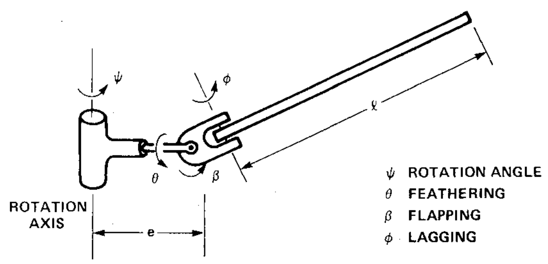

Fig. 1 Blade configuration.

this system are obtained by setting $\ddot{\theta}$ and $\dot{\theta}$ equal to zero; however, θ is retained as a rigid pitch for the blade.

1) Forced oscillations: assume the limit cycle solution as

$$\beta \approx \beta_c + a_1 \sin\psi + b_1 \cos\psi; \quad \phi \approx \phi_c + a_2 \sin\psi + b_2 \cos\psi \tag{5}$$

The higher harmonics $\sin 2\psi$, $\cos 2\psi$, etc., are neglected here. The β_c and ϕ_c represent the total center shifts, the mean angles about which limit cycle oscillations take place. Placing Eqs. (5) into the basic flap and lag equations and discarding the higher harmonic terms gives six nonlinear algebraic equations. These are solved numerically using the Newton-Raphson iterative technique.

2) Principal parametric resonance: for parametric instability in the first instability region,

$$\beta \approx \beta_c + a_1 \sin\frac{\psi}{2} + b_1 \cos\frac{\psi}{2}; \quad \phi \approx \phi_c + a_2 \sin\frac{\psi}{2} + b_2 \cos\frac{\psi}{2} \tag{6}$$

The higher harmonics $\sin\psi$, $\sin(3\psi/2)$, etc., are neglected. Placing these into the flap and lag equations and matching the constant $\sin(\psi/2)$, $\cos(\psi/2)$ terms of each equation results again in six nonlinear algebraic equations, which are solved by the Newton-Raphson method. The steady-state limit cycles occur at roughly twice the rotational speeds Ω of the forced oscillation resonances (i.e., $\approx 2\omega_\phi$) while the actual vibrations occur at roughly $\omega \approx \omega_\phi$.

3) Stability analysis: the nonlinear solutions obtained by the harmonic balance method are checked for stability by giving small perturbations to the steady solution and studying the growth rate of these disturbances under the assumption of slowly changing functions; see Bolotin[2] for details of the solution method. For the stability of the forced oscillations,

$$\beta = \beta_{c0} + \hat{\beta}_c(\psi) + [a_{10} + \hat{a}_1(\psi)]\sin\psi + [b_{10} + \hat{b}_1(\psi)]\cos\psi \tag{7a}$$

$$\phi = \phi_{c0} + \hat{\phi}_c(\psi) + [a_{20} + \hat{a}_2(\psi)]\sin\psi + [b_{20} + \hat{b}_2(\psi)]\cos\psi \tag{7b}$$

where β_{c0}, $a_{10} \ldots b_{20}$ is the steady solution for which a stability check is being made, and $\hat{\beta}_c, \hat{a}_1 \ldots \hat{b}_2$ are the time-dependent perturbations. Equations (7) are substituted into the basic flap-lag equations, and after retaining only linear terms in perturbations and their first-order derivatives, subtracting the steady solution, and matching the constant $\sin\psi$, and $\cos\psi$ terms, one gets six linear equations. These can be put into an eigenvalue problem, and the nature of the roots determines whether the solution is stable or not. On similar lines, a stability analysis for parametric resonance is made in Ref. 1.

Numerical results are discussed here for the following configuration:

$$\beta_s = 0.15, \phi_s = 0, \theta = 0, \frac{\omega_\beta}{\omega_\phi} = 0.71,$$

$$\frac{e}{\ell} = 0.067, \left(\frac{\omega_{\text{pend}}}{\omega_\phi}\right)^2 = \frac{3g}{2\ell\omega_\phi^2} = 0.088$$

where ω_β and ω_ϕ are the nonrotating flap and lag frequencies, and ω_{pend} is the pendulum frequency $\sqrt{3g/2\ell}$. This configuration represents a relatively flexible lag rotor, i.e., the case for which $\omega_\phi = 3.37\ \omega_{\text{pend}}$. However, in Ref. 1 the results are obtained for a wide range of stiffness parameters. The linear solution is obtained as a part of the nonlinear analysis by setting nonlinear terms in amplitudes a_1, b_1, a_2, b_2 to zero but still retaining higher-order terms in β_c and ϕ_c.

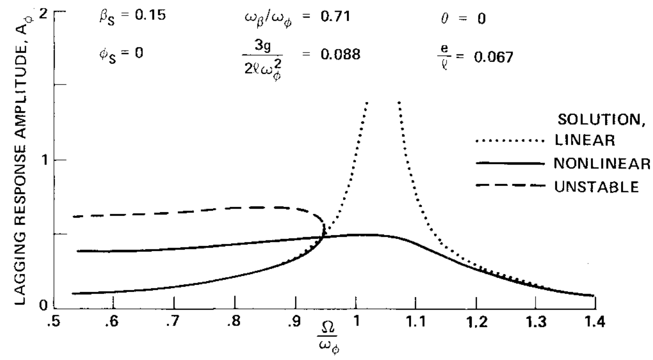

Fig. 2 Lead-lag response amplitude for forced oscillations.

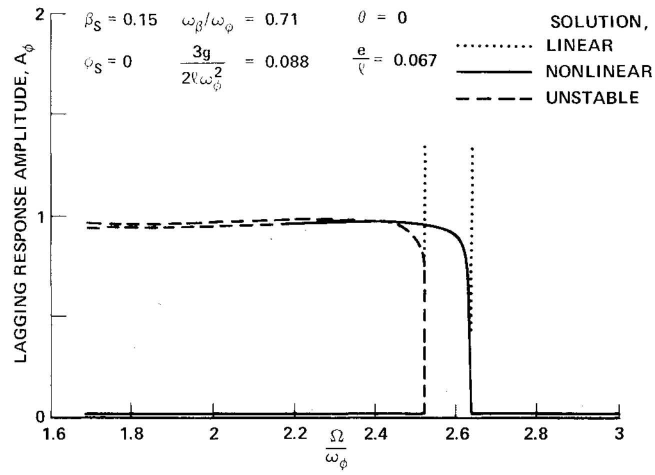

Fig. 3 Lead-lag response amplitude for parametric resonance.

In Fig. 2, the lagging response amplitude $A_\phi = \sqrt{a_2^2 + b_2^2}$ is plotted for different rotational speeds Ω/ω_ϕ for both linear and nonlinear forced oscillation solutions. One finds large differences between nonlinear and linear behavior, particularly after the amplitude starts increasing. At large amplitudes, the nonlinear resonance curves bend toward decreasing frequencies, portraying a typical softening spring-type system. Similar strongly nonlinear characteristics are also seen for flapping motion.[1] Thus, large-amplitude limit cycles are possible well below the lag frequency $\Omega \approx \omega_\phi$ if a large enough disturbance is given to the system.

Figure 3 presents the predominant lagging response for parametric resonance. Like forced oscillations, the nonlinear parametric resonance curves for larger amplitudes bend toward decreasing frequencies, again depicting a typical softening spring-type system.

It also is found that the inclusion of structural damping, which is in some way similar to aerodynamic damping, is quite effective in joining together the two instability branches in the overhang region for both forced oscillations and parametric resonances.[1] Also, in Ref. 1 the dynamic analysis results are discussed for various rotor configurations with the inclusion of aerodynamic forces. In conclusion, the results stress the importance of gravity forcing and the inclusion of nonlinear terms in the dynamics of a wind turbine.

References

[1] Chopra, I., "Nonlinear Dynamic Response of Wind Turbine Rotor," Sc. D. Thesis, Massachusetts Inst. of Technology, Cambridge, Mass., Feb. 1977.

[2] Bolotin, V. V., *Dynamic Stability of Elastic Systems*, Holden-Day Inc., San Francisco, Calif., 1964.